Quantum precession of cold neutron spin using multilayer spin splitters and a phase-spin-echo interferometer

Toru Ebisawa,[1] Seiji Tasaki,[1] Takeshi Kawai,[1] Masahiro Hino,[1] Norio Achiwa,[2] Yoshie Otake,[3] Haruhiko Funahashi,[4] Dai Yamazaki,[5] and Tsunekazu Akiyoshi[1]

[1]*Research Reactor Institute, Kyoto University, Kumatori, Osaka 590-0494, Japan*

[2]*Department of Physics, Kyushu University, Higashi-ku, Fukuoka 812-8581, Japan*

[3]*The Institute of Physical and Chemical Research (RIKEN), Mikazuki, Hyogo 679-5143, Japan*

[4]*Department of Physics, Kyoto University, Sakyo-Ku, Kyoto 606, Japan*

[5]*Department of Nuclear Engineering, Kyoto University, Sakyo-ku, Kyoto 606-5801, Japan*

(Received 26 December 1996; revised manuscript received 26 November 1997)

We demonstrate a method of inducing neutron spin rotation in a field-free region of space. A multilayer mirror (''spin splitter'') is used as an optically active element, providing a longer path length for one spin eigenstate of a polarized neutron than for the other. This produces a relative phase shift between the two eigenstates, which is interpreted, quantum mechanically, as precession of the neutron spin. We show that the spin precession of our technique is equivalent to Larmor precession in a magnetic field, though our method has no such classical analog and occurs on shorter (e.g., 20 nm) length scales. We also demonstrate a ''phase spin-echo'' interferometer based on a pair of multilayer spin splitters. [S1050-2947(98)03906-7]

PACS number(s): 03.75.Dg

I. INTRODUCTION

The spin of the neutron has been an interesting subject for many years, in large part because it provides a system that is at least superficially simple to consider. The proper description of the neutron spin is quantum mechanical, with a polarized neutron state described as a superposition of the eigenstates along some quantization axis of choice [1–5]. Precession of the neutron spin can then be thought of as the introduction of a relative phase shift between the spin eigenstates.

The quantum-mechanical interpretation of spin precession as a relative phase shift in the eigenstates is both useful and extremely general. On the one hand, it can be used to explain effects having clear classical analogs, such as Larmor precession in magnetic field, while on the other, it permits description of more general physical effects, including zero-field precession in the resonance spin-echo technique [6,7] and various neutron optical effects [8–12]. We refer to this general class of phenomena, particularly those without classical analogs, by the term ''quantum precession.''

Here, we demonstrate a type of neutron optical device, a ''multilayer spin splitter,'' that induces quantum precession of the neutron spin [8,9]. It consists of a magnetic multilayer mirror on top, followed by a gap layer and a nonmagnetic mirror. The top magnetic mirror reflects one spin eigenstate while the lower nonmagnetic mirror reflects the other eigenstate. The presence of the gap layer, however, creates a path-length difference for the two eigenstates. This results in a relative phase shift and, therefore, a quantum precession of the neutron spin.

This paper has four essential sections: (1) description of the structure and principles of the multilayer spin splitter; (2) demonstration of the operation of our spin splitters in a type of spin interferometer; (3) demonstration of the equivalency of the our quantum precession with Larmor precession in a magnetic field; and (4) demonstration of a type of ''phase-spin-echo'' neutron interferometer using a pair of multilayer spin splitters.

II. QUANTUM PRECESSION OF NEUTRON SPIN WITH MULTILAYER SPIN SPLITTER

Let us consider a neutron polarized in the (x,y) plane perpendicular to our quantization (z) axis. Equations (2.1) and (2.2) then express the neutron state $|S_{xy}(\phi)\rangle$ and the expectation value of the x-component $\langle S_x(\phi)\rangle$ [1–3], respectively:

$$|S_{xy}(\phi)\rangle = \frac{1}{2}\{|\uparrow_z\rangle + e^{i\phi}|\downarrow_z\rangle\} = e^{i\phi/2}\left\{\cos\left(\frac{\phi}{2}\right)|\uparrow_x\rangle - i\,\sin\left(\frac{\phi}{2}\right)|\downarrow_x\rangle\right\} \Big/ \sqrt{2} \tag{2.1}$$

$$\langle S_x(\phi)\rangle = \cos\,\phi, \tag{2.2}$$

where ϕ is the phase difference between the spin eigenstates. The validity of this description was demonstrated experimentally by Summhammer *et al.* using a silicon interferometer [4,5]. $\langle S_x(\phi)\rangle$ is measured by the coupled system of a $\pi/2$ flipper and an analyzer in a cold neutron spin interferometer, as used in conventional spin-echo technique.

The equation shows that the polarized neutron is described by the coherent superposition of the two spin eigenstates. ϕ gives both the relative phase shift between the spin eigenstates and the precession of the neutron spin. This permits an expanded concept of spin precession called quantum precession.

We consider a neutron optical device of a composite multilayer system consisting of a pair of parallel mirrors on

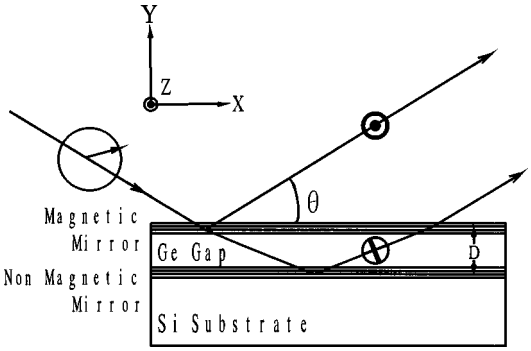

FIG. 1. Structure and principle of a multilayer spin splitter. The spin splitter consists of a magnetic mirror on top, followed by a gap layer and a nonmagnetic mirror on a well-polished silicon substrate. An additional phase difference ϕ between the two spin eigenstates is produced due to the presence of the gap layer.

either side of a gap layer. The multilayer system is evaporated on a well polished silicon substrate, as shown in Fig. 1. We call this a multilayer spin splitter. The top mirror of the multilayer spin splitter is a magnetic mirror with high reflectivity ($\geqslant 90\%$) for the $+1/2$ spin component of the neutron and with sufficiently low reflectivity for the $-1/2$ spin component. On the other hand, the back mirror is a nonmagnetic mirror with high reflectivity ($\geqslant 90\%$) for the $-1/2$ spin component. In principle, either a multilayer monochromator mirror or a total reflection mirror can be used for the magnetic mirror and the nonmagnetic mirror. Germanium is used for the gap layer.

When a neutron polarized in the (x,y) plane is incident on a multilayer spin splitter, the $+1/2$ spin component of the neutron is reflected by the top magnetic mirror while the $-1/2$ spin component is reflected by the nonmagnetic mirror on the bottom. An additional phase shift between the spin eigenstates is produced by the effective gap thickness D, which is taken to be equal to the thickness of the gap layer added to half the total thickness of the two reflection mirrors on the both sides [13]. The phase shift originates from the different path lengths between the two subbeams with the spin eigenstates.

Neutron optical phenomena in a multilayer system may be evaluated by considering the component of the neutron momentum normal to the mirror surface [14], since only the normal component undergoes the change of the potential on the boundaries of the multilayer system. The additional phase shift ϕ is given by the following equations, taking $n_\perp(\theta)$ as the average refractive index of the effective gap layer for the normal component of the neutron momentum,

$$\phi = \frac{4\pi D n_\perp(\theta)\sin\theta}{\lambda}, \tag{2.3}$$

$$n_\perp(\theta) = \frac{K_\perp}{k_\perp} = \left[1 - \frac{N b_c}{\pi}\left(\frac{\lambda}{\sin\theta}\right)^2\right]^{1/2} \tag{2.4}$$

where θ is the neutron incident angle, λ the neutron wavelength, N and b_c are the average atomic density and coherent scattering length of the effective gap layer, respectively. $K_\perp$ and $k_\perp$ are the wave numbers for the normal component of the neutron wave vector in the effective gap layer and air, respectively.

When we use a pair of multilayer monochromator mirrors with period d as the two reflection mirrors of our spin splitter, Eq. (2.3) is transformed into Eq. (2.5) taking account of the Bragg condition for the monochromator mirrors, $\lambda = 2d\sin\theta$.

$$\phi = \frac{2\pi D n_\perp(\theta)}{d}. \tag{2.5}$$

Equation (2.5) shows that only short distances are needed for our quantum precession because d and $n_\perp$ are typically 100 to 200 Å and 0.95 to 0.6, respectively.

When we change the neutron incident angle θ onto a multilayer spin splitter by $\Delta\theta$, the phase shift also changes. The change $\Delta\phi$ is given by the equation, assuming $\theta \ll 1$ and $\Delta\theta \ll 1$,

$$\begin{aligned}\Delta\phi &= \frac{4\pi D}{\lambda}\{n_\perp(\theta)\sin\theta - n_\perp(\theta+\Delta\theta)\sin(\theta+\Delta\theta)\} \\ &\approx -\frac{4\pi D\Delta\theta}{n_\perp(\theta)\lambda}.\end{aligned} \tag{2.6}$$

The above relation between the change of quantum precession using a spin splitter and an angular shift of the incident neutrons is useful for the demonstration experiments of the equivalency between our quantum precession and Larmor precession in a magnetic field. We note that the change of the quantum precession is in inverse proportion to the refractive index $n_\perp(\theta)$.

The quantum precession originates from the different path lengths between the spin eigenstates. In contrast, Larmor precession in a magnetic field originates from the different momenta of the eigenstates depending on the Zeeman splitting between them, in spite of their identical geometrical path length. The quantum-mechanical description predicts these precessions to be equivalent.

The quantum precession using a multilayer spin splitter has features different from conventional Larmor precession, such as it is free from magnetic field and needs a very short distance for precession. In addition, the two partial waves by the multilayer spin splitter have a transverse separation as well as a longitudinal one (Fig. 1), which may be useful for studies of neutron transverse and longitudinal coherence.

It should be noted that in the case of the silicon interferometer a whole neutron has no precession, because the spin precession of the forward beam of the interferometer after the superposition is complementary to that of the deviated beam, and the precessions of the two subbeams mutually cancel out [3,5]. With a multilayer spin splitter, on the other hand, a whole neutron may precess because the multilayer spin splitter has a high reflectivity and has just one beam after the coherent superposition, different from the silicon interferometer.

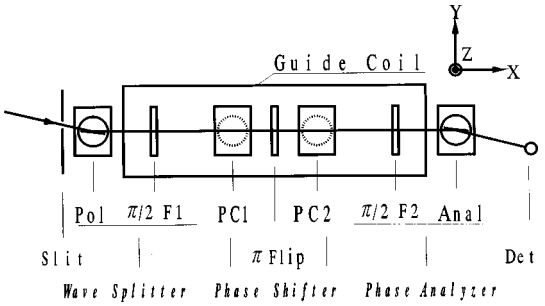

FIG. 2. Structure of a new cold neutron spin interferometer. The basic structure, indicated by the solid lines, is optically analogous to a conventional spin-echo system with a vertical precession field. ''Pol'' indicates the polarizer, ''Flip'' the flipper, ''PC1'' the first precession coil, ''PC2'' the second precession coil, ''Anal'' the analyzer, and ''Det'' the neutron detector. The two goniometers indicated by dotted lines are mounted in the PC1 and PC2 magnetic fields for setting up neutron mirrors.

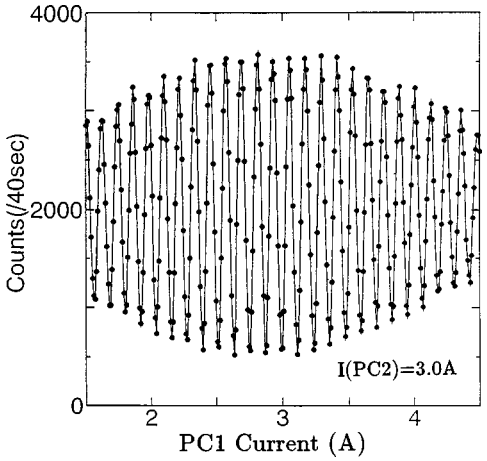

FIG. 3. Measured spin-echo profile. The profile is measured as a function of PC1 coil current at a fixed PC2 current of 3 A. One period of the profile corresponds to a change of 2π in the Larmor precession in the magnetic field.

III. METHOD OF PERFORMANCE TEST ON MULTILAYER SPIN SPLITTERS

We use an interferometer [15] to demonstrate that our quantum precession is equivalent to Larmor precession in a magnetic field. This interferometer is optically analogous to a spin-echo system with transverse precession field [10,16]. However, using the concept of quantum precession, we may describe it as a spin interferometer. This is because it includes all the usual components of an interferometer (a wave splitter, a wave combiner, a phase sensitive device, and a phase shifter) all operating on the neutron spin.

The basic structure of the spin interferometer for cold neutrons is shown in Fig. 2. Rectangles indicate coils and circles goniometers. Optical elements include a polarizer, two $\pi/2$ flippers, a π flipper, two vertical precession fields, a vertical guide field, and an analyzer. The flippers are identical Mezei coils, while the vertical fields are produced by solenoids. All fields are controlled by changing the currents.

Considering this as an interferometer, the polarizer and the first $\pi/2$ flipper splits the incident neutron into two partial waves corresponding to the spin eigenstates. The waves are superposed and the phase shift between them is analyzed by the second $\pi/2$ flipper and the analyzer. A relative phase shift is introduced by varying the current in either precession field. The π flipper acts to compensate for the Larmor precession in the guide field by satisfying the spin-echo condition.

Our spin interferometer has several notable features that are different from the conventional spin-echo systems [16] though, as pointed out by Mezei, a quantum-mechanical description is needed even in the conventional system to calculate the behavior of the neutron spin with high accuracy [17]. Our system is also different from the spin interferometer proposed by Baryshevskii *et al.* [18] for precise measurements of refractive indices using ultracold neutrons. The notable and different features of our system include: (a) The magnetic mirrors used in the spin interferometer function in a very low magnetic field of 5 Oe [19]. (b) The entire system operates with a very small magnetic field so the spin precession in the system has a very small rotation number. This means the interferometer is relatively easy to fabricate and gives spin-echo profiles with high visibility. (c) Many kinds of spin-dependent optical devices can be mounted in the spin interferometer. We can control the phase and states of the two partial waves with respect to each other. This will allow us to do many experiments using cold neutron spin interferometry.

The first spin interferometer was set up at the *CN*1 beam port of the Kyoto University research reactor with a cold source [20] in the autumn of 1995. The incident monochromatic neutron beam was obtained using a pair of multilayer monochromators (Ni/Ti, $d=115$ Å) in a nondispersive $(+-)$ arrangement. The incident neutron wavelength was 8.0 Å and the wavelength resolution about 4.5%.

Another spin interferometer was installed at the *C*3-1-2 beam port of JRR-3 reactor with cold source in the beginning of 1996. The incident neutrons are monochromatized and bent by 24 degrees by four sequential Bragg reflections using four multilayer monochromators arranged in $(++++)$ configuration [21]. The neutron wavelength was 12.6 Å and the wavelength resolution 3.5%.

Figure 3 shows a typical spin-echo profile of the spin interferometer, taken as a function of the coil current PC1 of the first precession field at constant coil current for PC2 of 3.0 A of the second precession field. The profile shows the Larmor precession of the neutron spin depending on PC1

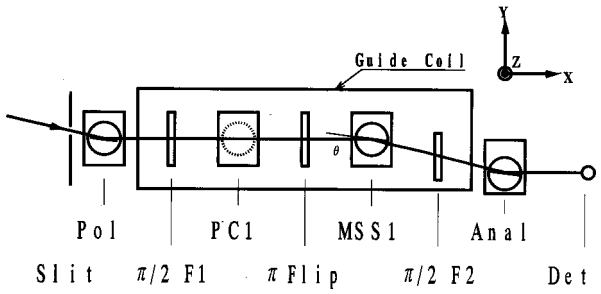

FIG. 4. Arrangement for the performance test of a multilayer spin splitter. The spin splitter is set up on the goniometer in the second precession field (PC2). The spin-echo profile is measured as a function of PC1 coil current for a fixed PC2 coil current.

current. One period of the profile corresponds to the Larmor precession of 2π. The visibility of the spin-echo profile is 75%, which may be improved by optimization of the system.

The arrangement for the performance tests of the multilayer spin splitters is shown in Fig. 4. A multilayer spin splitter was set up on the goniometer in the magnetic field by PC2 coil so that the neutron incident angle can be scanned around the design angle θ. The spin-echo profiles were measured as a function of PC1 coil current for a fixed current of PC2 coil.

In order to verify experimentally the characteristics of the quantum precession by a multilayer spin splitter, we demonstrate that the change $\Delta\phi_P$ of the quantum precession by an angular shift $\Delta\theta$ [given by Eq. (2.6)] can be compensated by an identical change $\Delta\phi_L$ of the Larmor precession in the PC1 magnetic field. We, however, usually cannot obtain a spin echo profile with observable contrast around the conventional spin-echo condition, because the phase difference ϕ caused by a multilayer spin splitter entails a dispersion, $\delta\phi$, due to the wavelength distribution $\delta\lambda$ and the divergence angle, $\delta\theta$, of the incident neutrons. The dispersion of the phase difference, $\delta\phi$, is evaluated, neglecting the dependency of $n_\perp(\theta)$ on θ and λ,

$$\delta\phi = \frac{4\pi D n_\perp(\theta)\sin\theta}{\lambda}\{-(\delta\lambda/\lambda)+(\cot\theta)\delta\theta\}. \quad (3.1)$$

As $(D\sin\theta)/\lambda$ increases the dispersion $\delta\phi$ becomes larger and larger depending on $\delta\lambda/\lambda$ and $(\cot\theta)\delta\theta$. In this case, the wavelength dispersion dominated. A large dispersion will average out the contrast of the spin-echo profile.

We could compensate for the dispersion of the phase difference $\delta\phi_P$ originating from the wavelength distribution $\delta\lambda$ of the incident neutrons, and restore the contrast by using an extra Larmor precession in the PC1 magnetic field, which means an excess Larmor precession deviating from the spin-echo condition for the system without multilayer spin splitter. Expressing the extra Larmor precession for a wavelength λ by ϕ_L, the dispersion of the phase shift $\delta\phi_P$ and that of the Larmor precession $\delta\phi_L$ are given by Eq. (3.2) and Eq. (3.3), respectively, for a wavelength $\lambda+\delta\lambda$ deviating by $\delta\lambda$ from the center of the wavelength λ, to lowest order in $\delta\lambda/\lambda$:

$$\delta\phi_P = 4\pi D n_\perp(\theta)\sin\theta\left\{\frac{1}{\lambda}-\frac{1}{\lambda+\delta\lambda}\right\} \approx \frac{4\pi D n_\perp(\theta)\sin\theta}{\lambda}(\delta\lambda/\lambda), \quad (3.2)$$

$$\delta\phi_L = \frac{\phi_L}{\lambda}\{(\lambda+\delta\lambda)-\lambda\} = \phi_L(\delta\lambda/\lambda), \quad (3.3)$$

where the sign of Eq. (3.3) is reversed owing to the π flipper.

The restoration of the contrast of spin-echo profile depends on the cancellation of $\delta\phi_P$ by $\delta\phi_L$. The maximum contrast of the profile should be expected for the following reduction of the Larmor precession in PC1 magnetic field from the conventional spin-echo condition.

$$\phi_L = -\frac{4\pi D n_\perp(\theta)\sin\theta}{\lambda}. \quad (3.4)$$

It should be noted that the dependence of the dispersions on $\delta\theta$ and on terms of higher order in $\delta\lambda/\lambda$ are neglected in the above echo condition, which is different from the conventional spin-echo or phase-echo phenomena satisfying the perfect echo condition.

IV. RESULTS OF THE PERFORMANCE TESTS OF MULTILAYER SPIN SPLITTERS

Two kinds of performance tests were done: (a) Contrast measurements of spin-echo profiles for multilayer spin splitters: Data of spin-echo profiles were taken as a function of PC1 coil current for a multilayer spin splitter mounted in the fixed magnetic field of PC2. We measured the contrast of spin echo profiles depending on the current of PC1 coil. The results were compared with the values evaluated from Eq. (3.4). (b) Shift measurements of spin-echo profiles by sequential angle displacements of multilayer spin splitter: First we measured spin-echo profiles changing neutron incident angle θ on the multilayer spin splitter with a step of 0.03° from the design angle. Next we evaluated the shifts of the spin echo profiles for the angle displacements, which correspond to the change of the Larmor precession. Last the shifts were compared with the phase difference $\Delta\phi$ given by Eq. (2.6), which corresponds to the change of the quantum precession by the angle displacement.

A. Fabrication of multilayer spin splitters

The multilayer spin splitter was designed and fabricated using techniques from cold neutron optics with multilayer mirrors [13,22–25]. Using multilayer mirrors, we can create a square potential system of one dimension appropriate for the study of neutron optics and interferometry. Layers of ferromagnetic material enable us to control the potential height depending on the spin state of a neutron. Magnetic

TABLE I. Design parameters of multilayer spin splitters fabricated. The abbreviation of PG/G2/NT, for example, expresses a multilayer spin splitter which consists of a Pe/Ge magnetic multilayer on top, followed by a Ge gap layer with a thickness of 2000 Å and Ni/Ti multilayer on bottom.

Multilayer spin splitter	Magnetic mirror	Ge gap layer (Å)	Nonmagnetic mirror	Effective gap thickness (Å)
P/G2/N	Pe: 700 Å	2000 Å	Ni: 700 Å	2700
PG/G2/NT	Pe/Ge: 100 Å×14	2000 Å	Ni/Ti: 100 Å×14	3700
PG/G5/NT	Pe/Ge: 100 Å×14	5000 Å	Ni/Ti: 100 Å×14	6700

multilayer mirrors that function in a very low field of 5 Oe [19] are very useful for cold neutron spin interferometry.

The multilayer spin splitter is deposited on well polished silicon substrates, which are placed in a magnetic field of about 100 Oe. Layers of permalloy-45 used for magnetic layers saturate their magnetization in a low magnetic field of 5 Oe, having a saturated magnetic flux density of 1.6 T. We prepared three types of multilayer spin splitters, as listed in Table I. Gap layers were 2000 or 5000 Å of Ge. The mirrors were both total reflection mirrors (operating at 1.17°) and multilayer structures (operating at 1.8°).

In the case of P/G2/N, we use two total reflection mirrors of Permalloy-45 (Pe) and nickel (Ni) with layer thickness of 700 Å in order to reflect the two spin states, and a germanium (Ge) gap layer with thickness of 2000 Å. In the case of PG/G2/NT and PG/G5/NT, we use two multilayer mirrors of Pe/Ge and Ni/Ti. The magnetic multilayer mirror Pe/Ge $=100\ \text{Å}\times 14$ consists of 7 bilayers of Permalloy-45 and germanium layers with a layer thickness of 100 Å in optical length, and has a reflectivity of about 90%. The nonmagnetic mirror is a conventional Ni/Ti multilayer, which has the same optical design as the magnetic multilayer. The actual thicknesses of the deposited layers are 152 Å (Pe), 132 Å (Ni), 108 Å (Ge), and 98 Å (Ti), which were measured using a quartz-crystal monitor. The gap layer thicknesses of germanium are 2000 Å and 5000 Å for G2 and G5, respectively. Effective gap thickness are evaluated from the layer structure of the spin splitter, as described above.

B. Contrast measurements of spin-echo profiles

Figure 5 shows the spin-echo profiles as a function of PC1 current measured for the multilayer spin splitters (a) P/G2/N, (b) PG/G2/NT, and (c) PG/G5/NT, which were set up in the fixed magnetic field of PC2. The abscissa indicates the PC1 coil current and the ordinate the neutron counts. The currents of PC2 coil were at values of 1.8, 2.4, and 4.3 A for P/G2/N, PG/G2/NT, and PG/G5/NT, respectively. The neutron incident angle for P/G2/N is 1.17°, which is smaller than the critical total reflection angle of 1.20°. The neutron incident angle for PG/G2/NT and PG/G5/NT is 1.80°, which corresponds to the Bragg angle of the multilayer monochromator mirrors.

When the current of the PC1 coil is equal to that of the PC2 coil, the conventional spin-echo condition is satisfied for the Larmor precession in the magnetic field. On the other hand, the multilayer spin splitter brings some large dispersion of the phase difference, as described by Eq. (3.1). We, therefore, cannot observe any good contrast of the spin-echo profile due to the large dispersion. However, the contrast is restored when the current of the PC1 coil is reduced to less than that of the PC2 coil, as given by Eq. (3.4). The measured recovery of the contrast is related to the echo phenomenon between the phase difference and the Larmor precession, as previously described by Eqs. (3.2), (3.3), and (3.4).

In order to evaluate quantitatively the contrast of the spin-echo profiles, we fit the measured results using

$$Y=a\ \cos\left\{2\pi\ \frac{(X-c)}{b}\right\}\exp\left\{-\frac{(X-d)^2}{2e^2}\right\}+f, \quad (4.1)$$

where Y is the neutron count and X the PC1 current. Coefficients of $a-f$ are the fitting parameters. The ratio, a/f, gives the maximum contrast of the spin-echo profile. Parameter b indicates the change of PC1 coil current corresponding to one period of the spin-echo profile, which is equivalent to one rotation of the Larmor precession: $b=0.116$ means that PC1 coil current of 0.116 A causes Larmor precession by

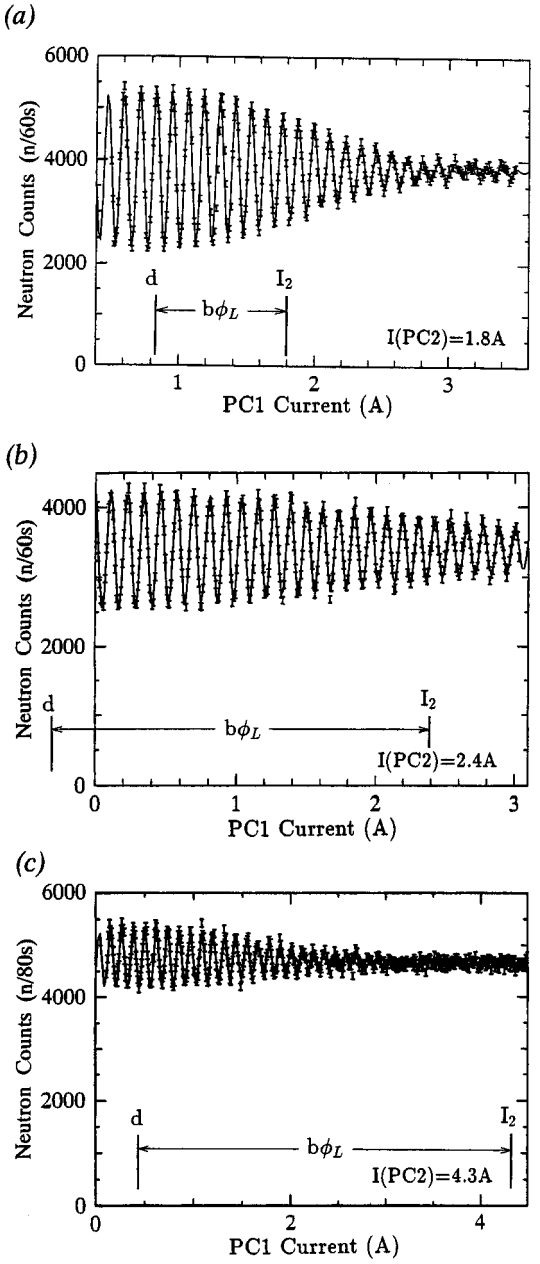

FIG. 5. Spin-echo profiles for three multilayer spin splitters: (a) P/G2/N with fixed PC2 current of 1.8 A, (b) PG/G2/NT with fixed PC2 current of 2.4 A, and (c) PG/G5/NT with fixed PC2 current of 4.3 A. Recovery of the contrast of the spin-echo profile was observed in lower current region of coil PC1 as compared to the fixed PC2 coil current. Solid lines are fits based on Eq. (4.1). I_2 is the constant current of coil PC2 and d the measured current of coil PC1 that gives the best recovery. b is the change of the PC1 coil current corresponding to one rotation of the Larmor precession. The measured rotation reduction ϕ_L of the Larmor precession is evaluated from the data.

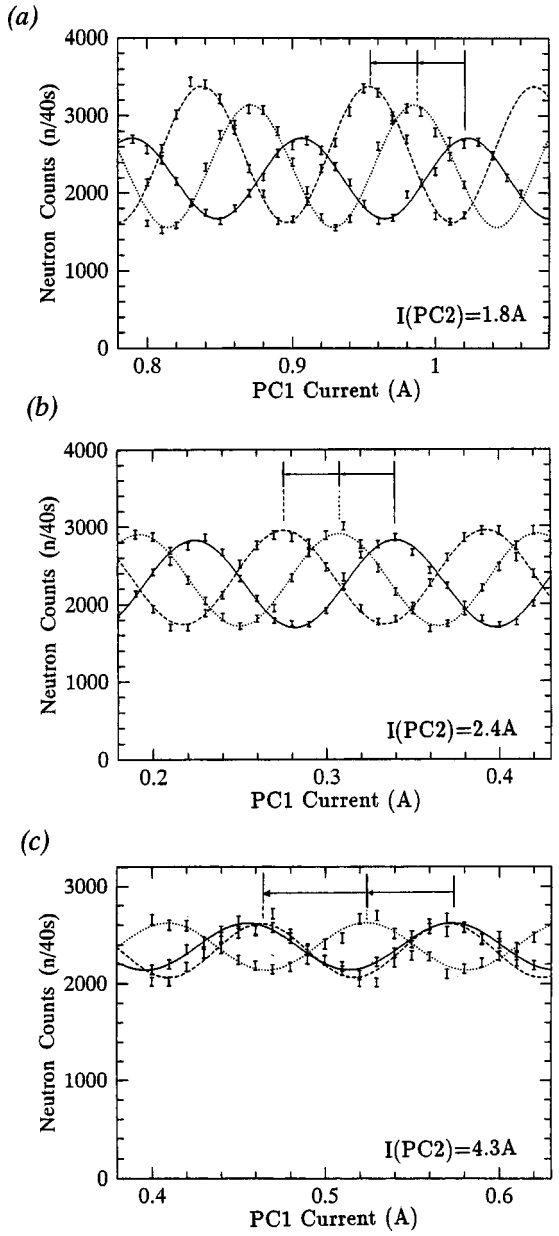

FIG. 6. Spin-echo profiles for a sequential angular shift of 0.03°. (a) is for P/G2/T, (b) for PG/G2/NT, and (c) for PG/G5/NT. The solid, dotted, and broken lines are fits for angular shifts of 0°, 0.03°, and 0.06°, respectively. The data demonstrate that the spin-echo profiles shift to a lower current region with larger angular shift.

2π. Parameter d indicates the PC1 current, which gives the maximum contrast of the profile. The fitting results are shown in Table II.

The conventional spin-echo condition for the system without multilayer spin splitter requires that the current of PC1 coil is equal to that of the PC2 coil. Expressing the fixed current of PC2 coil by I_2 the measured rotation reduction, ϕ_L, of the Larmor precession from the conventional spin echo condition is evaluated by

$$\phi_L=\frac{(I_2-d)}{b}. \tag{4.2}$$

From Eqs. (3.4) and (4.2) we can evaluate the effective gap thicknesses D, as given in Table II. These evaluated thicknesses of the effective gaps (Table II) are qualitatively consistent with the design values (Table I). The tendency for the measured values to be larger than the design values is probably due to some nonuniformity of the magnetic field produced by PC1 coil. This is because the deterioration of the contrast by the nonuniformity is reduced with smaller current of PC1 coil and results in a smaller apparent value d in measurement. This then gives an apparent larger value of effective gap thickness D. The rather large discrepancy in the case of PG/G2/NT might partially be due to the low accuracy of the profile measurement.

This recovery of the contrast demonstrates that the quantum precession induced by the multilayer spin splitter is equivalent to the magnetic Larmor precession. Furthermore, the recovery phenomena enable us to observe the interference pattern by the superposition of the two partial waves with the large transverse separation in space. Using this phenomenon we will have a suitable tool for coherency studies of two neutron partial waves with transverse separation.

The following experiments were made in the current region of PC1 coil, which gives a maximum contrast of the spin echo profile.

C. Shift measurement of spin-echo profiles

Spin-echo profiles were measured for sequential angular shifts of 0.03°. Figure 6 shows typical measured spin-echo profiles for the three multilayer spin splitters (a) P/G2/N, (b) PG/G2/NT, and (c) PG/G5/NT. The abscissa is the current of coil PC1. The lines indicate the fit results for the standard case without angular shift (solid line), for an angular shift of 0.03° (dotted line), and for an additional angular shift of 0.03° (broken line). The data show at a glance that the spin-echo profiles shift to lower current region with larger angular shift, as described by Eq. (2.6) and the changes of the quantum precession caused by the angular shifts are compensated by the changes of the Larmor precession in the magnetic field produced with coil PC1.

In order to quantitatively evaluate the measured shifts of spin-echo profiles, the measured data were fit by a least-squares method using the following function:

TABLE II. Results from a least-squares fit to the data using Eq. (4.1).

Multilayer spin splitter	a	b	c	d	e	f	PC2 Current (A)	Evaluated effective gap thickness (Å)
P/G2/N	1540±10	0.116±0.0001	0.833	0.83±0.00	0.99	3820±4	1.8	3300±4
PG/G2/NT	867±24	0.116±0.0001	−0.007	−0.29±0.21	2.27	3400±4	2.4	5100±400
PG/G5/NT	564±11	0.116×0.0001	0.038	0.44±0.08	1.21	4740±4	4.3	7320±150

TABLE III. Results from a least-squares fit to the data using Eq. (4.3).

Multilayer spin splitter	Angle (deg)	a	b	c	d
P/G2/N	0.99	878±14	0.117±0.001	0.729±0.001	2250±11
	1.02	921±14	0.117±0.001	0.759±0.001	2450±11
	1.05	564±15	0.115±0.001	0.805±0.001	2490±12
	1.08	971±15	0.117±0.001	0.846±0.001	2520±11
	1.11	963±11	0.116±0.001	0.875±0.001	2550±8
	1.14	719±16	0.115±0.001	0.913±0.001	2530±12
	1.17	878±15	0.116±0.001	0.954±0.001	2500±11
	1.20	790±14	0.114±0.001	0.986±0.001	2350±11
	1.23	524±10	0.116±0.001	1.022±0.001	2190±17
PG/G2/NT	1.70	617±15	0.115±0.001	0.194±0.001	2370±11
	1.73	631±14	0.111±0.001	0.238±0.001	2390±10
	1.76	604±14	0.117±0.001	0.275±0.001	2340±10
	1.79	592±14	0.115±0.001	0.307±0.001	2310±11
	1.82	563±11	0.116±0.001	0.340±0.001	2260±8
PG/G5/NT	1.61	180±13	0.115±0.002	0.182±0.003	1850±9
	1.64	282±14	0.112±0.002	0.262±0.003	2200±10
	1.67	268±15	0.120±0.002	0.325±0.003	2310±11
	1.70	289±11	0.116±0.001	0.401±0.002	2400±8
	1.73	286±14	0.115±0.002	0.462±0.002	2320±11
	1.76	241±14	0.115±0.002	0.524±0.002	2380±11
	1.79	239±15	0.118±0.002	0.573±0.002	2380±11

$$Y = a\,\cos\left\{2\pi\,\frac{(X-c)}{b}\right\} + d, \tag{4.3}$$

where Y is the neutron count and X the current of coil PC1 and coefficients a, b, c, and d are the fitting parameters. The ratio a/d gives the visibility of the contrast of the spin-echo profile. Parameter b is the current change of PC1 coil corresponding to one period of the spin-echo profile, i.e., Larmor precession of 2π. The shift of the spin-echo profile is given by the change of parameter c. Fit results are given in Table III. When we change the incident angle by $\Delta\theta$, the measured shift of spin-echo profile is evaluated from the change of parameter c. The fit gives b to be approximately 0.116 A, which is nearly equal to that of the previous measurements (Table II).

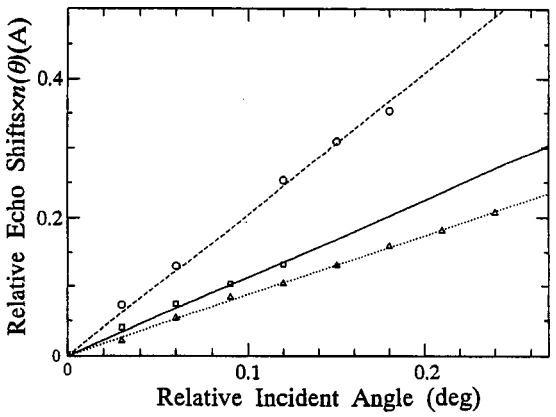

FIG. 7. Summarized data between angular shift and measured shift of the spin-echo profiles. Dotted, solid, and broken lines are fits to the data for P/G2/N, PG/G2/NT, and PG/G5/NT, respectively, using Eq. (2.6).

Equation (2.6) predicts a relationship between the angular shift and the quantum precession. If we consider the angular shift as Δc, then Eq. (2.6) becomes $\Delta\phi = 2\pi\Delta c/b$. This is plotted in Fig. 7 for the three multilayer spin splitters. The ordinate is the shift of spin-echo profiles divided by the averaged refractive index $n_\perp(\theta)$ of the effective gap layer. The abscissa is the angular shift. The points are the shifts from Table III, while the lines show the expected relationship from Eq. (2.6). There is excellent agreement taking gap thicknesses of 2750 Å(P/G2/N), 3480 Å(PG/G2/NT), and 6320 Å(PG/G5/NT), in good agreement with the expected values (Table I). The figure shows that the shifts of the echo profile depend on the sequential angular shifts and the effective gap thicknesses as predicted from Eq. (2.6). Applying Eq. (2.3) gives that we induced quantum precessions of 6.8 rotations (P/G2/N), 15.9 rotations (PG/G2/NT), and 28.5 rotations (PG/G5/NT), at angles of 1.17°, 1.80°, and 1.80°, respectively.

These results demonstrate that the multilayer spin splitter creates a quantum precession, which is equivalent to the Larmor precession. It should be noted that the quantum precession is free from the magnetic field and needs a very small distance for neutron spin precession, and that these characteristics are quite different from both the conventional Larmor precession and the zero-field precession of the resonance spin echo.

V. PERFORMANCE TESTS OF A PHASE-SPIN-ECHO INTERFEROMETER

Taking into account the equivalency of quantum precession by multilayer spin splitter and Larmor precession, we

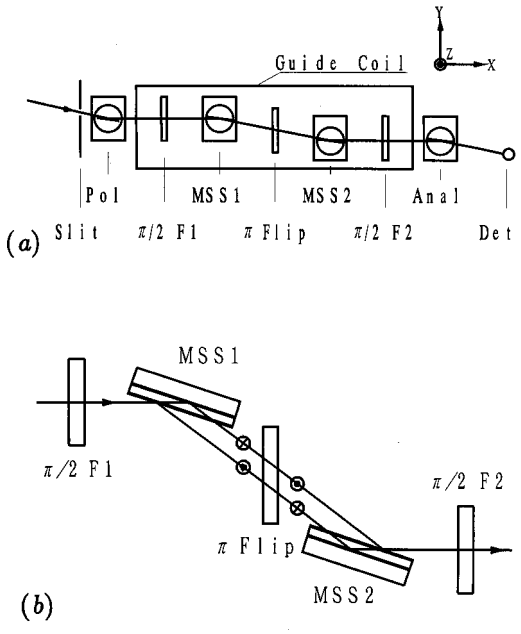

FIG. 8. (a) An arrangement of a phase–spin-echo interferometer using two identical multilayer spin splitters, which are mounted in the first precession field PC1 and the second precession field PC2 in the Jamin configuration. (b) Illustration of the simultaneous occurrence of phase-echo and spin-echo phenomena. The phase echo requires a π turn flipper as well as a pair of identical multilayer spin splitters.

suggest a multilayer spin interferometer with a pair of identical multilayer spin splitters. This is optically quite analogous to a conventional spin-echo spectrometer, as proposed previously [8]. We mount two identical spin splitters, parallel to each other, in a Jamin configuration, as shown in Fig. 8(a), so the pair of multilayer spin splitters satisfies the phase-echo condition [13] and the spin-echo condition [16] simultaneously.

The simultaneous occurrence of the two echo phenomena is illustrated in Fig. 8(b). The first multilayer spin splitter causes an additional phase difference between the two spin eigenstates given by Eq. (2.3). The π flipper reverses the states of the two subbeams. The reversed subbeams are reflected and superposed by the second spin splitter. As a result, the path length difference caused by the first multilayer spin splitter is compensated by the identical path length difference of the second one. We call this geometrical compensation a phase echo. The neutron polarization status after the reflection by the second spin splitter is restored completely by the phase-echo and the spin-echo phenomena for which we require a π flipper. This restoration occurs for all incident neutrons independent of their angular and wavelength dispersion. So we call this system a phase-spin-echo interferometer.

Our phase-spin-echo system may be compared with previous work, including both the phase-echo experiments of Clothier *et al.* [26] and Rauch [27] and the more conventional spin-echo system. In the first work, the two partial waves have identical path lengths and wavelength-dependent phase differences are created by inserting a material with nonzero susceptibility on one path. The induced phase difference is then removed by using a material having susceptibility of the opposite sign. Likewise, the conventional spin-echo system may be regarded as a kind of phase-echo from a quantum-mechanical viewpoint. In this case the phase difference between the two spin eigenstates, having identical geometrical path length, is caused by their different momenta due to Zeeman splitting. The phase difference is then compensated using a central π flipper. From a quantum-mechanical viewpoint, all of these systems (phase spin echo, phase echo, and spin echo) are very similar.

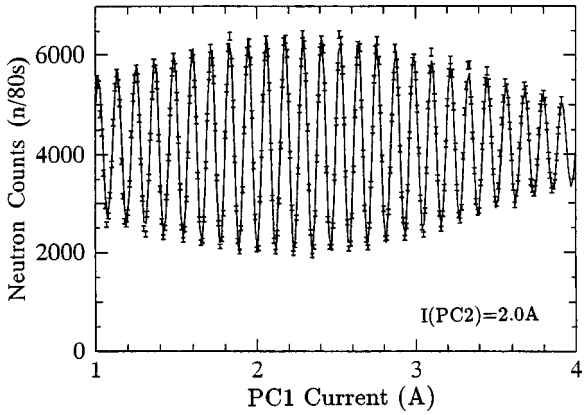

FIG. 9. Measured spin-echo profile for a phase–spin-echo interferometer composed of PG/G5/NT. The contrast of the spin-echo profiles is restored nearly perfectly by the simultaneous occurrence of the phase- and spin-echo phenomena.

The measured spin-echo profile for the phase-spin-echo interferometer is shown in Fig. 9. Comparison of Fig. 9 and Fig. 6 demonstrates a remarkable improvement of the contrast of the spin-echo profiles by the simultaneous occurrence of the phase-echo and spin-echo phenomena.

We can measure the quantum precession induced by a multilayer spin splitter with good contrast using a phase-spin-echo interferometer. Figure 10 shows typical results for a phase-spin-echo interferometer composed of PG/G2/NT. Fit results are given in Table IV, which are in qualitative agreement with those in Table III.

A long term goal of this work is to develop a high-resolution phase-spin-echo interferometer. A gap layer thickness of 1 mm corresponds to about 10^5 spin rotations and

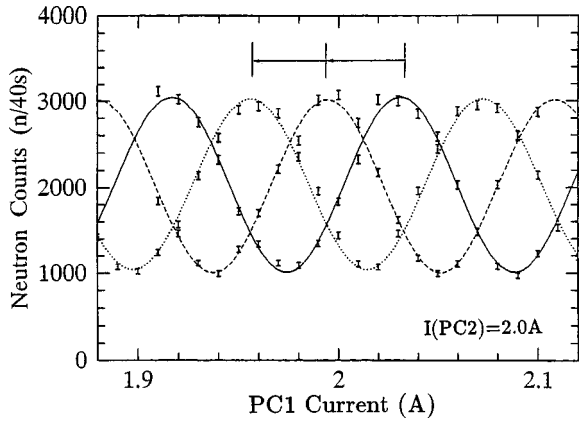

FIG. 10. Spin-echo profiles of PG/G2/NT for a sequential angular shift of 0.03°. The solid, broken, and dotted lines are fits for angular shifts of 0°, 0.03°, and 0.06°, respectively. We observe shifts of the spin-echo profiles similar to those shown in Fig. 6.

TABLE IV. Results from a least-squares fit to the data using Eq. (4.3).

Multilayer spin splitter	Angle (deg)	*a*	*b*	*c*	*d*
PG/G2/NT	1.70	1020±14	0.115±0.001	1.958±0.001	2070±11
	1.73	1060±15	0.113±0.001	2.000±0.001	2040±11
	1.76	1020±14	0.115±0.001	2.031±0.001	2030±10
	1.79	991±10	0.117±0.001	2.073±0.001	2030± 7
	1.82	1010±13	0.114±0.001	2.109±0.001	2000±11

would allow extremely precise measurements with a very compact setup. However, there are some technical challenges involved in fabricating such a device that must be overcome first. Furthermore, we should investigate the coherency characteristics of the partial waves with transverse and longitudinal separations.

VI. CONCLUSION

Quantum precession was defined as a phase shift originating from the quantum-mechanical description of spin. Quantum precession of neutron spin by a multilayer spin splitter was proposed based on the coherent superposition of the two spin eigenstates. The multilayer spin splitter consists of a magnetic mirror on top, followed by a nonmagnetic gap layer and a nonmagnetic mirror. The nonmagnetic gap layer produces a phase shift between the two spin eigenstates, which causes a quantum precession.

Two kinds of performance tests of multilayer spin splitters were carried out using a cold neutron spin interferometer: contrast measurements of spin-echo profiles for multilayer spin splitters and shift measurements of spin-echo profiles by sequential angle displacement of a multilayer spin splitter. These experiments clearly demonstrated that the effect of the quantum precession can be compensated by that of the Larmor precession. The quantum precession has the advantages that it is free from magnetic field and needs only a very short distance for the spin precession. The two partial waves with spin eigenstates have a transverse separation, as well as a longitudinal one, which increase proportionally to the gap thickness. This separation of the partial waves will be useful for the transverse and longitudinal coherency studies of neutron waves.

We have developed a phase-spin-echo interferometer using a pair of multilayer spin splitters, arranged in the spin interferometer to satisfy the phase echo and the spin echo simultaneously. The phase-spin-echo interferometer provides extremely good contrast owing to the simultaneous occurrence of phase-echo and spin-echo phenomena. A compact spin-echo spectrometer with high resolution by quantum precession is proposed as an application of a phase-spin-echo interferometer.

ACKNOWLEDGMENTS

We would like to thank Professor Akira Masaike for stimulating discussions and Dr. Alfred Baron for valuable discussions and a careful reading of the manuscript. This work was supported in part by the Inter-University Program for Common Use JAERI Facility and by the Common Use Program for KUR Facility, and financially supported by the Grant-in-Aid for Scientific Research from the Ministry of Education, Science and Culture in Japan (Project Nos. 04244103 and 08404014).

[1] E. P. Wigner, Am. J. Phys. **31**, 6 (1963).
[2] A. Zeilinger, Z. Phys. B **25**, 97 (1976).
[3] A. Zeilinger, *Neutron Interferometry*, edited by U. Bonse and H. Rauch (Clarendon Press, Oxford, 1979), p. 241.
[4] J. Summhammer, G. Badurek, H. Rauch, and U. Kischko, Phys. Lett. **90A**, 110 (1982).
[5] J. Summhammer, G. Badurek, H. Rauch, U. Kischko, and A. Zeilinger, Phys. Rev. A **27**, 2523 (1983).
[6] R. Gähler and R. Golub, Z. Phys. B **65**, 269 (1987).
[7] R. Gähler, R. Golub, and T. Keller, Physica B **180&181**, 899 (1993).
[8] T. Ebisawa, H. Funahashi, S. Tasaki, Y. Otake, T. Kawai, M. Hino, N. Achiwa, and T. Akiyoshi, J. Neutron Research **4**, 157 (1996).
[9] T. Ebisawa, S. Tasaki, T. Kawai, M. Hino, N. Achiwa, T. Akiyoshi, Y. Otake, and H. Funahashi, J. Phys. Soc. Jpn. Suppl. A **65**, 66 (1996).
[10] N. Achiwa, M. Hino, S. Tasaki, T. Ebisawa, T. Kawai, and T. Akiyoshi, J. Phys. Soc. Jpn. Suppl. A **65**, 183 (1996).
[11] M. Hino, N. Achiwa, S. Tasaki, T. Ebisawa, T. Kawai, and T. Akiyoshi, J. Phys. Soc. Jpn. Suppl. A **65**, 281 (1996).
[12] T. Ebisawa, D. Yamazaki, S. Tasaki, T. Kawai, M. Hino, N. Achiwa, T. Akiyoshi, and Y. Otake, J. Phys. Soc. Jpn. (to be published).
[13] H. Funahashi, T. Ebisawa, T. Haseyama, M. Hino, A. Masaike, Y. Otake, T. Tabaru, and S. Tasaki, Phys. Rev. A **54**, 649 (1996).
[14] F. V. Sears, *Neutron Optics* (Oxford University, London, 1989), p. 66.
[15] T. Ebisawa, S. Tasaki, T. Kawai, M. Hino, D. Yamazaki, N. Achiwa, and T. Akiyoshi (unpublished).
[16] F. Mezei, Z. Phys. **255**, 146 (1972).
[17] F. Mezei, in *Imaging Processes and Coherence in Physics*, edited by M. Schlenker *et al.*, Lecture Notes in Physics Vol. 112 (Springer-Verlag, Heidelberg, 1979), p. 283.
[18] V. G. Baryshevskii, S. V. Cherepitsa, and A. L. Frank, Phys. Lett. A **153**, 299 (1991).

[19] T. Kawai, T. Ebisawa, S. Tasaki, Y. Eguchi, M. Hino, and N. Achiwa, J. Neutron Research **5**, 123 (1997).
[20] T. Kawai, T. Ebisawa, T. Akiyoshi, and S. Tasaki, Ann. Rep. Res. React. Inst. Kyoto University **23**, 158 (1990).
[21] T. Ebisawa, S. Tasaki, Y. Otake, H. Funahashi, K. Soyama, N. Torikai, and Y. Matsushita, Physica B **213&214**, 901 (1995).
[22] S. Yamada, T. Ebisawa, N. Achiwa, T. Akiyoshi, and S. Okamoto, Ann. Rep. Res. React. Inst. Kyoto University **11**, 8 (1978).
[23] T. Ebisawa, N. Achiwa, S. Yamada, T. Akiyoshi, and S. Okamoto, J. Nucl. Sci. Technol. **16**, 647 (1979).
[24] S. Tasaki, T. Ebisawa, T. Akiyoshi, T. Kawai, and S. Okamoto, Nucl. Instrum. Methods Phys. Res. A **344**, 501 (1995).
[25] S. Tasaki, T. Kawai, and T. Ebisawa, J. Appl. Phys. **78**, 2398 (1995).
[26] R. Clothier, H. Kaiser, S. A. Werner, H. Rauch, and H. Wöwitsch, Phys. Rev. A **44**, 5357 (1991).
[27] H. Rauch (unpublished).